Chemistry & Biology, Vol. 12, 703–715, June, 2005, ©2005 Elsevier Ltd All rights reserved. DOI 10.1016/j.chembiol.2005.04.019

$S1P_1$-Selective In Vivo-Active Agonists from High-Throughput Screening: Off-the-Shelf Chemical Probes of Receptor Interactions, Signaling, and Fate

Euijung Jo,[1] M. Germana Sanna,[1] Pedro J. Gonzalez-Cabrera,[1] Shobha Thangada,[2] Gabor Tigyi,[3] Daniel A. Osborne,[4] Timothy Hla,[2] Abby L. Parrill,[4] and Hugh Rosen[1,*]

[1]Department of Immunology
The Scripps Research Institute
10550 North Torrey Pines Road, ICND 118
La Jolla, California 92037

[2]Center for Vascular Biology
Department of Cell Biology
University of Connecticut Health Center
Farmington, Connecticut 06030

[3]Department of Physiology
University of Tennessee Health Science Center
Memphis, Tennessee 38163

[4]Department of Chemistry
University of Memphis
Memphis, Tennessee 38152

Summary

The essential role of the sphingosine 1-phosphate (S1P) receptor $S1P_1$ in regulating lymphocyte trafficking was demonstrated with the $S1P_1$-selective nanomolar agonist, SEW2871. Despite its lack of charged headgroup, the tetraaromatic compound SEW2871 binds and activates $S1P_1$ through a combination of hydrophobic and ion-dipole interactions. Both S1P and SEW2871 activated ERK, Akt, and Rac signaling pathways and induced $S1P_1$ internalization and recycling, unlike FTY720-phosphate, which induces receptor degradation. Agonism with receptor recycling is sufficient for alteration of lymphocyte trafficking by S1P and SEW2871. $S1P_1$ modeling and mutagenesis studies revealed that residues binding the S1P headgroup are required for kinase activation by both S1P and SEW2871. Therefore, SEW2871 recapitulates the action of S1P in all the signaling pathways examined and overlaps in interactions with key headgroup binding receptor residues, presumably replacing salt-bridge interactions with ion-dipole interactions.

Introduction

Sphingosine 1-phosphate (S1P), through its high affinity G protein-coupled receptors $S1P_{1-5}$, is a physiological mediator with widespread effects upon multiple physiological systems [1–9]. It regulates heart rate [10], coronary artery blood flow [11], blood pressure [12], endothelial integrity in lung [13, 14], and, most recently, has been shown to regulate the recirculation of lymphocytes [15–19]. Many of the physiologically relevant functions occur in the low nanomolar range, including activation of endothelial nitric-oxide synthase [20, 21], vasorelaxation [22], and inhibition of thymic egress and lymphocyte recirculation [15]. Free plasma levels of S1P are tightly regulated by protein binding to albumin and high-density lipoprotein and by abundant extracellular lipid phosphatases to avoid the deleterious effects of systemic S1P receptor subtype activation at high concentrations of ligand, such as bradycardia and coronary artery vasospasm [11, 23]. The choice of S1P, through its receptor $S1P_1$, as an acute regulator of the number of blood lymphocytes may represent an interesting evolutionary choice by the immune system, which evolved after the circulatory system. This has been supported by receptor-selective agonists [24] and selective receptor deletional studies [25, 26]. The discovery of potent synthetic agonists of the S1P receptors such as FTY720-phosphate (now in clinical trials for prevention of renal allograft rejection) has rapidly extended the field into therapeutics, whereas many of the key features of system regulation at a molecular level remain inadequately understood.

We have recently shown that SEW2871, originally identified by high-throughput screening of commercial chemical libraries with a 384-well-format FLIPR calcium-flux assay, can cause lymphopenia via an $S1P_1$-dependent mechanism [24]. It was also idenfified by high-throughput screening with GTPγS binding assay [27]. In the present study, we examined the signaling pathways and receptor fate in cells activated by SEW2871 and its structurally related analogs. Upon agonist stimulation, $S1P_1$ has been reported to internalize and colocalize with endocytic vesicles and lysosomes [28, 29]. The high-affinity ligand S1P induces the recycling of $S1P_1$ back to the plasma membrane via the endosomal pathway [28]. However, FTY720-phosphate was recently reported to induce internalization and degradation of $S1P_1$, resulting in receptor downregulation and lymphocyte sequestration in vivo [25, 30]. Therefore, it was of interest to examine whether the mode of action of SEW2871 produces functional antagonism or long-term activation of postreceptor signaling mechanisms. This study could allow us to narrow down the signals that need to be considered in unraveling the control of lymphocyte recirculation.

Furthermore, the two-site binding model for S1P [31] raised questions about the extent to which receptor-ligand interactions for the tetraaromatic structures overlapped those for S1P, particularly with regard to recapitulating any headgroup interactions that might be essential for proper conformational changes in the receptor in response to agonist binding. We therefore used a combination of computational modeling, receptor mutagenesis, and chemical ligands to examine the role of headgroup interactions in $S1P_1$ signaling by agonists of different structures.

Understanding the signaling properties of the S1P receptors within the context of both model cell systems in vitro and within tissues in vivo will have an important prospective impact on S1P pathway therapeutics, relevant to immune, cardiovascular, and respiratory diseases as well as cancer [1, 32, 33].

*Correspondence: hrosen@scripps.edu

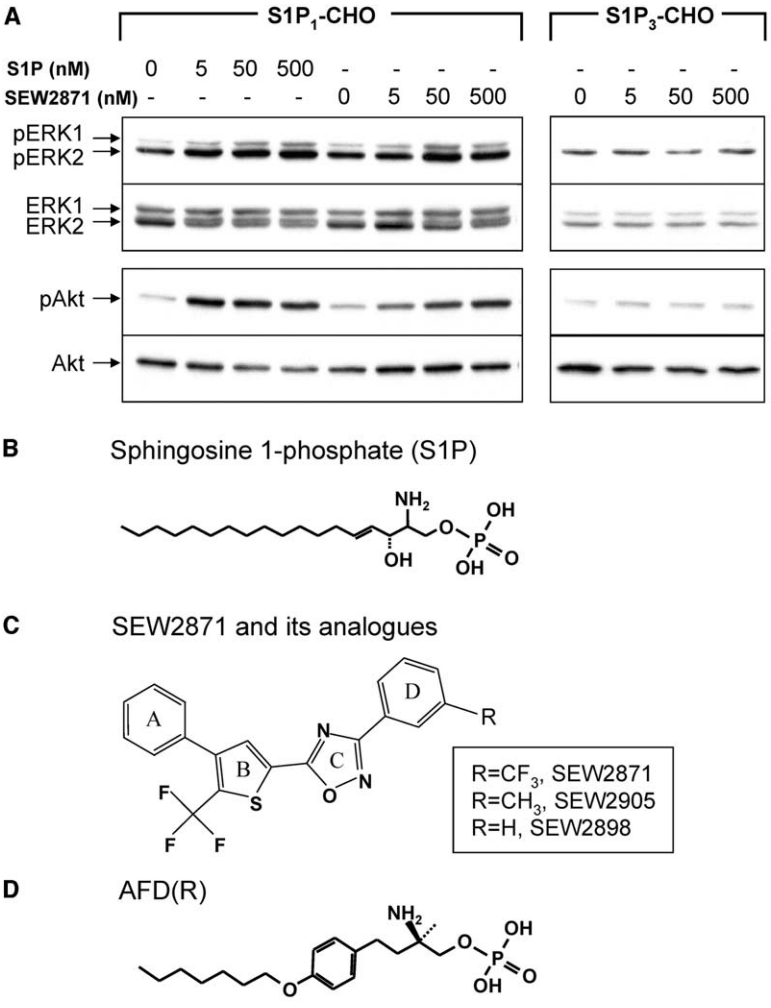

Figure 1. Both S1P and SEW2871 Induce Phosphorylation of ERK1/2 and Akt in CHO Cells Stably Transfected with $S1P_1$

(A) CHO cells stably transfected with either $S1P_1$ or $S1P_3$ were serum starved and stimulated with either S1P or SEW2871 at the indicated concentrations for 5 min. Western blot analyses of phospho-ERK1/2, total ERK1/2, phospho-Akt, and total Akt levels were shown. Data are representative autoradiograms of several experiments. Vector-transfected CHO cells contained only the minimal levels of pERK1/2 and pAkt (data not shown).

(B) Structure of sphingosine 1-phosphate (S1P).

(C) SEW2871 and its analogs.

(D) AFD(R).

Results

Both S1P and SEW2871 Induce Activation of MAP Kinase and Akt Pathways

S1P has been reported to activate mitogen-activated protein kinases (MAP kinases) in many systems [34–40]. Therefore, we examined the phosphorylation of extracellular signal-regulated kinase 1 (ERK1) and ERK2 in CHO cells stably transfected with $S1P_1$. Phosphorylation of both ERK1 and ERK2 was increased in a concentration-dependent manner after stimulation of cells with S1P for 5 min (Figure 1A). SEW2871, a $S1P_1$ receptor-selective agonist, also induced concentration-dependent phosphorylation of ERK1 and ERK2. Both S1P and SEW2871 induced phosphorylation of Akt (Figures 1A, 1B, and 1C), confirming that Akt is involved in the downstream signaling events initiated by $S1P_1$ [21, 41–43].

SEW2871 is an $S1P_1$-selective full agonist (inducing responses equivalent to 100% of those seen with the physiological ligand S1P) in GTPγS binding, calcium flux, and cell migration assays [24]. $S1P_1$ selectivity of SEW2871 action on kinase activation is shown in Figure 1A. ERK1/2 and Akt phosphorylation was observed in response to SEW2871 stimulation in $S1P_1$-CHO cells but not $S1P_3$-CHO cells (Figure 1A). However, S1P, a non-selective agonist, induced phosphorylation of ERK1/2 and Akt in both $S1P_1$-CHO and $S1P_3$-CHO cells (data shown for $S1P_1$-CHO cells only).

The relative potencies of S1P, AFD(R), and SEW2871 (Figures 1B–1D) for kinase activation and GTPγS binding were determined by EC_{50} measurement. S1P was more potent in inducing ERK/Akt phosphorylation than SEW2871. For instance, S1P at 5 nM was sufficient to induce maximal phosphorylation of Akt, whereas 500 nM of SEW2871 was needed to induce the same level of Akt phosphorylation (Figure 1A). This relative difference in potency on downstream signal generation was even more obvious when comparing AFD(R) to SEW2871. As shown in Figures 2A–2C, AFD(R) induced phosphorylation of ERK and Akt at ligand concentrations that were three to four orders of magnitude lower than SEW2871 (Table 1). This suggested that ligand binding and downstream signaling were greatest for AFD(R), intermediate for S1P, and least for SEW2871 at subnanomolar ligand concentrations. However, all three ligands were full agonists inducing phosphorylation of these signaling molecules to the same extent, provided

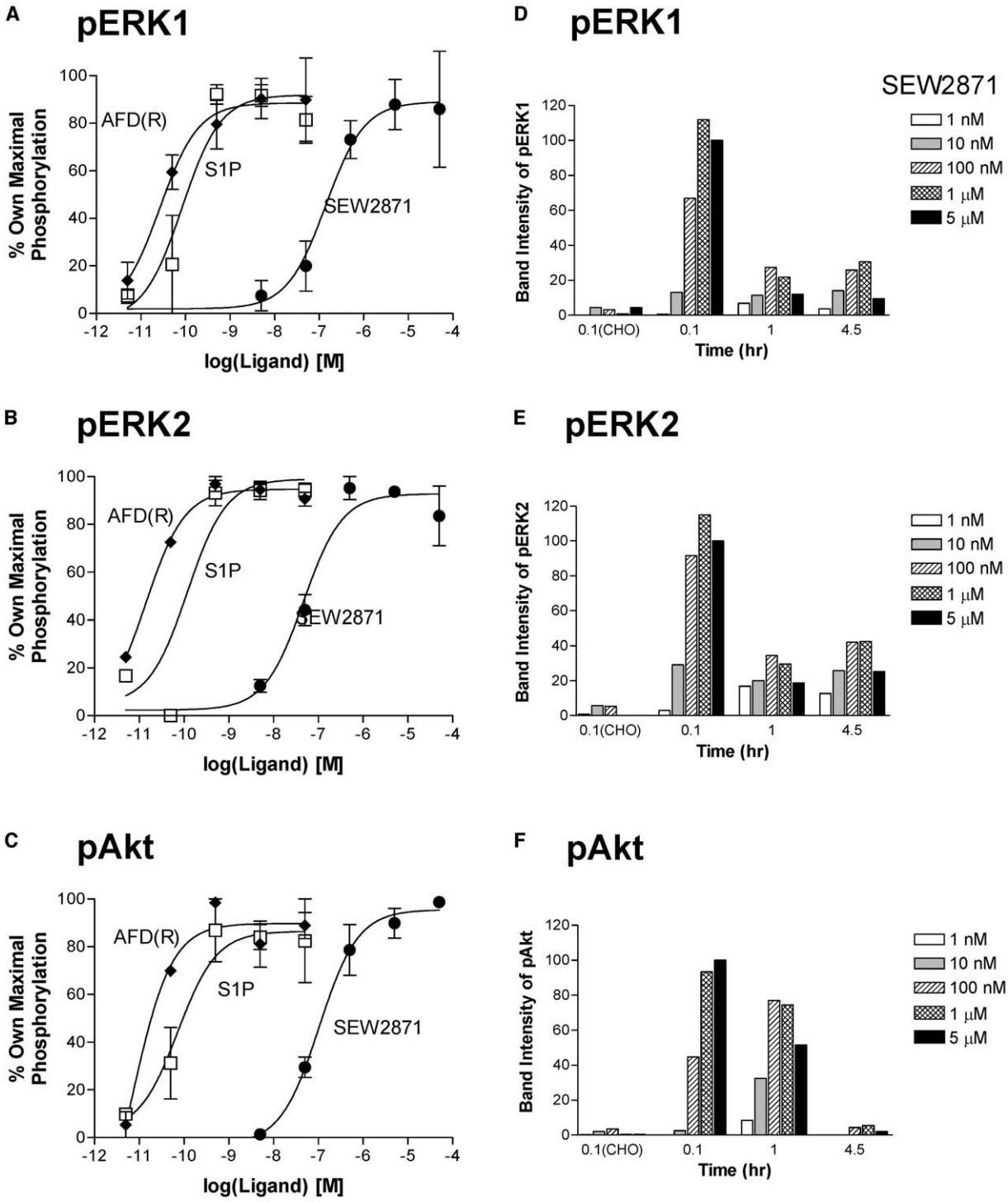

Figure 2. Agonist Dose Response Curves of Phosphorylation of ERK1/2 and Akt upon Stimulation with S1P$_1$ Agonists

(A–C) CHO cells stably transfected with S1P$_1$ were serum starved and stimulated with AFD(R), S1P, or SEW2871 at the indicated concentrations for 5 min. The band intensities of phosphoproteins were integrated, normalized against total ERK or Akt, and expressed as percentage of maximal phosphorylation upon AFD(R) (♦), S1P (□), and SEW2871 (●) stimulation. Data represent mean ± SD of three independent experiments.

(D–F) Time course of phosphorylation of ERK1/2 and Akt upon stimulation with SEW2871. CHO cells stably transfected with S1P$_1$ were serum starved and stimulated with SEW2871 at the indicated concentrations (1 nM to 5 μM) for 5 min, 1 hr, and 4.5 hr. Band intensities corresponding to (D) pERK1, (E) pERK2, and (F) pAkt were quantitated by image analysis and normalized against total ERK or Akt. Data are expressed as percentage of the level of phosphorylation obtained at 5 μM SEW2871 for 5 min stimulation. Nontransfected CHO cells were included as negative control.

Table 1. EC_{50} Values (nM) of $S1P_1$ Agonists from GTPγ^{35}S Assay and Downstream Phosphorylation of Akt, ERK1, and ERK2

	GTPγ^{35}S	pAkt	pERK1	pERK2
AFD(R)	0.032 ± 0.006 (n = 3)	0.007 ± 0.005	0.03 ± 0.01	0.01 ± 0.005
S1P	0.4 ± 0.24 (n = 6)	0.07 ± 0.04	0.09 ± 0.04	0.07 ± 0.04
SEW2871	13.8 ± 8.3 (n = 3)	104 ± 34	141 ± 62	46 ± 20

Data for GTPγ^{35}S assay are average ± standard error from three to six experiments, and data for kinase assay are average ± standard error from triplicate experiments.

that high enough ligand concentrations were used. The relative affinities of $S1P_1$ for these ligands were examined in a competition assay by measuring displacement of [^{33}P]-labeled S1P by cold S1P and AFD(R). The IC_{50} values were 2.2 ± 0.5 nM for S1P and 5.5 ± 2.0 nM for AFD(R). The IC_{50} for SEW2871 was reported to be 37 nM [27].

We next examined the time course of phosphorylation of ERK1, ERK2, and Akt for AFD(R), S1P, and SEW2871. The kinetics of phosphorylation was similar for all three ligands, and data is shown for SEW2871 (Figures 2D–2F). As shown in Figures 2D–2E, both ERK1 and ERK2 phosphorylation was maximal at 5 min stimulation, and the level of phospho-ERK decreased with time, but the level of phospho-ERK remained elevated for at least 4.5 hr of stimulation. On the other hand, Akt phosphorylation was near maximal level up to 1 hr of stimulation with SEW2871 but decreased to basal level by 4.5 hr (Figure 2F).

To help define the G proteins that are involved in the agonist-induced Akt and ERK phosphorylation, we examined the effect of $G_{i/o}$ inhibitor pertussis toxin (PTx) [44]. Preincubation of the $S1P_1$-CHO cells with PTx completely inhibited both ERK and Akt phosphorylation in response to AFD(R) and SEW2871 (Figure 3A). The PTx-induced inhibition of the phosphorylation was almost complete when stimulated with S1P (Figure 3A). This suggests that all the agonists tested share the ERK and Akt signaling pathways through activation of $G_{i/o}$ protein and that $G_{i/o}$ protein activation is formally upstream of kinase recruitment.

Both S1P and SEW2871 Induce Activation of Rac GTPase

Small GTPases of the Rho family, including Rac1, Rho, and Cdc42, play an important role in cytoskeletal changes and cell motility in response to receptor stimulation [45, 46]. S1P has been reported to elicit either stimulatory or inhibitory effects on cell migration, depending on cell type and availability of S1P receptor subtypes [47, 48]. We have examined whether S1P activates Rac1 in CHO cells stably transfected with $S1P_1$. In order to pull down only the active (GTP bound) Rac with GSH-Sepharose beads, we utilized GST-tagged p21 binding domain of p21-activated protein kinase 1 (PAK1) [47]. After S1P stimulation of $S1P_1$-CHO cells for 2–5 min, Rac was activated significantly at 2 min, compared to the negative control (Figure 3B). SEW2871 also activated Rac both at 2 min and 5 min, suggesting that Rac activation is a common signaling pathway of $S1P_1$ agonist stimulation. Rac activation was increased in an agonist-concentration-dependent manner, and the potency was higher for S1P than SEW2871. S1P at 50 nM caused maximal Rac activation, whereas 5 μM of SEW2871 was required to induce the maximal Rac activation. This difference in potency on Rac activation is consistent with that on ERK and Akt phosphorylation.

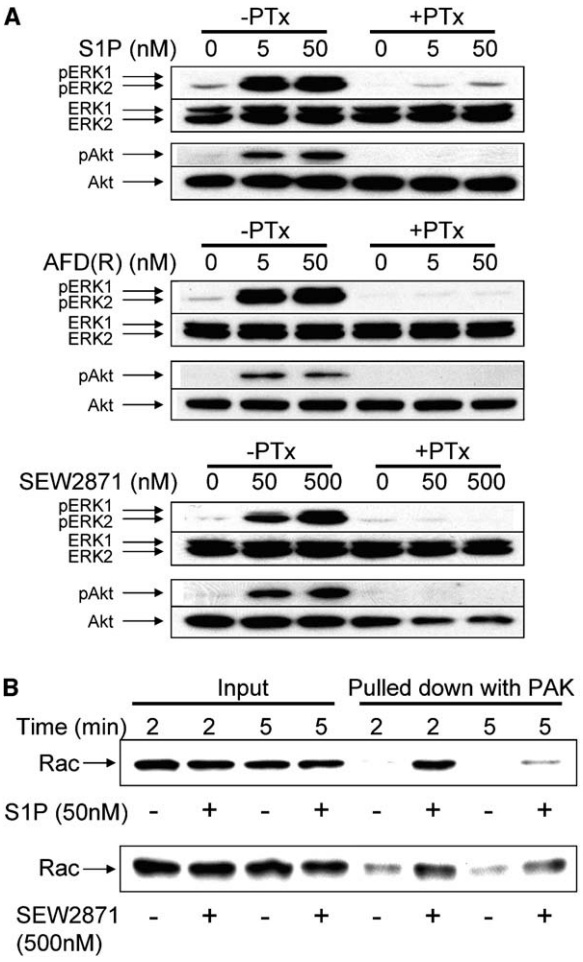

Figure 3. $S1P_1$-Mediated ERK1/2 and Akt Phosphorylation is $G_{i/o}$ Dependent

(A) ERK1/2 and Akt phosphorylation upon stimulation with S1P, AFD(R), and SEW2871 is $G_{i/o}$ dependent. $S1P_1$-CHO cells were incubated with pertussis toxin at the final concentration of 100 ng/ml for 3 hr prior to agonist stimulation and analyzed for pERK1/2 and pAkt levels.

(B) Activated Rac pull-down assay. CHO cells stably transfected with $S1P_1$ were serum starved and stimulated with S1P at 50 nM or SEW2871 at 500 nM for 2 and 5 min. Active (GTP bound) Rac was pulled down with GST-PBD (p21 binding domain of PAK1) and GSH-Sepharose beads. Western blot analysis of the eluents with anti-Rac antibody is shown.

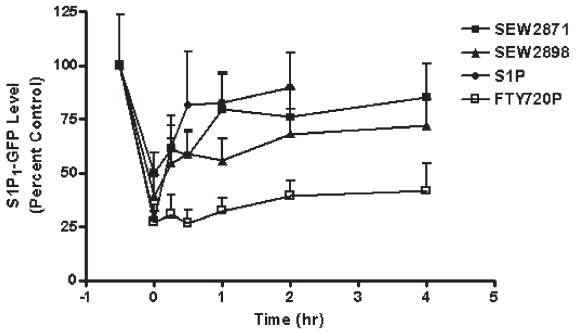

Figure 4. S1P$_1$ Internalization and Recycling Back to Plasma Membrane

HEK293 cells that were stably transfected with GFP-tagged S1P$_1$ were serum starved, pretreated with cycloheximide (15 μg/ml) for 30 min, and stimulated with 100 nM S1P, FTY720-phosphate, 500 nM SEW2871, or SEW2898 for 30 min. Cells were washed and incubated for indicated time points. The fluorescence of the recycled receptor at each time point was quantified and expressed as percent control. Data represent mean ± SD of fluorescence intensities of ten randomly selected fields.

In addition, we have observed cytoskeletal changes, such as ruffle formation and increased stress fiber formation, upon SEW2871 stimulation of S1P$_1$-CHO cells, which is consistent with the Rac activation (see Figures S1 and S2 available with this article online).

Both S1P and SEW2871 Induce S1P$_1$ Receptor Internalization and Recycling

S1P$_1$ has been reported to internalize and colocalize with endocytic vesicles, caveolae, and lysosomes upon S1P stimulation and to recycle back to the plasma membrane [20, 28, 29, 49]. We have examined whether SEW2871 also induces S1P$_1$ receptor internalization and recycling in HEK293 cells that are stably transfected with GFP-tagged S1P$_1$. SEW2871 (500 nM) induced S1P$_1$ receptor internalization to the similar extent as S1P (100 nM) (Figure 4). Both SEW2871 (500 nM) and S1P (100 nM) induced the receptors to recycle back to the plasma membrane when cells were washed and treated with cycloheximide (Figure 4). The receptor recycling was observed as early as 15 min, and it was increased slowly up to 4 hr. On the other hand, FTY720-phosphate induced S1P$_1$ receptor internalization without recycling (Figure 4).

Activation of S1P$_1$ by SEW2871 Requires Polar Receptor Residues that Support Salt-Bridge Interactions with the S1P Headgroup

It has been reported that the basic side chains of Arg120 (3.28) and Arg292 (7.34) of the S1P$_1$ receptor support electrostatic interactions with the phosphate group of S1P, whereas the acidic side chain Glu121 (3.29) ion pairs with the ammonium moiety of S1P, leading to S1P headgroup interaction with its receptor [31]. SEW2871 does not contain a charged headgroup, although it was possible that the dipole moment of its trifluoromethyl group could potentially substitute for the headgroup interaction with S1P$_1$. We therefore examined the contributions of the "headgroup" interactions by computational modeling of S1P$_1$-SEW2871 complex as well as the receptor interaction with SEW2871 analogs without the trifluoromethyl group. SEW2905 is the methyl replacement of the trifluoromethyl on the phenyl ring of SEW2871 (D ring in Figure 1C), whereas SEW2898 has no substituent on the D ring of SEW2871 (Figure 1C).

The optimal position of SEW2871 in the S1P$_1$ receptor places the D ring trifluoromethyl group in close proximity to R3.28 (120), E3.29 (121), and R7.34 (292) (Figure 5A). The electronegative fluorine atoms favorably interact with the cationic R3.28 and R7.34 residues, whereas the less electronegative carbon of the trifluoromethyl group interacts with the anionic E3.29 residue. Multiple hydrophobic residues form close contacts with the aromatic rings of SEW2871, including phenylalanine residues from TM3 (125), TM5 (273), and TM7 (296) as well as a tryptophan residue from TM5 (269). SEW2905 adopts a similar position (Figure 5B), although the interactions with R3.28, E3.29, and R7.34 are not as favorable. SEW2898 (Figure 5C) is displaced toward the extracellular loops relative to the positions of the other two ligand positions in S1P$_1$. On the other hand, AFD(R), an S1P analog containing a phosphate group and an ammonium moiety (Figure 1D), showed a favorable headgroup interaction with S1P$_1$, as predicted (Figure 5D).

The optimal location of SEW2871 in the S1P$_2$ receptor model is very poor, with docked energies approximately 10 kcal/mol less favorable than the S1P$_1$ complexes. No interactions are observed with the polar residues R3.28 (108), E3.29 (109), or K7.34 (269) (data not shown). Interactions with aromatic residues in TM3 (125), TM6 (246, 250), and TM7 (273) are also not as favorable as in S1P$_1$. The poor interactions in the S1P$_2$ receptor can be partially attributed to replacement of arginine with lysine at position 7.34. An arginine residue at position 7.34 (292) is unique to S1P$_1$, with lysine occurring in the S1P$_2$ (269) and S1P$_3$ (279) receptors, and uncharged residues occurring in the S1P$_4$ (G288) and S1P$_5$ (Q288) receptors.

We then measured the contributions of the headgroup interactions by both mutational analysis and the testing of structural analogs of SEW2871 in order to confirm our computational models. We examined downstream kinase activities upon stimulation of site-directed mutant receptors that define the S1P headgroup interactions to see if the mutant receptors show abolished or significantly diminished S1P responses observed in both wild-type and control mutant receptors. CHO cells were transiently transfected with four site-directed mutant receptors, R3.28A, E3.29A, R7.34A, and N101(2.60)K. The N2.60K mutant was included as a positive control because N2.60 is located just outside the ligand binding pocket. This N2.60K mutant receptor was shown to behave similarly to the wild-type receptor by radioligand binding, ^{35}S-GTPγS binding, and receptor-internalization assays [31].

CHO cells transfected with the wild-type receptor or the control N2.60(101)K mutant responded to S1P stimulation, resulting in phosphorylation of ERK2 and Akt (Figure 6A). However, the ion-pairing defective mutants, R3.28(120)A, E3.29(121)A, and R7.34(292)A, showed decreased phosphorylation of ERK1/2 and Akt compared to the wild-type or N2.60K, suggesting that im-

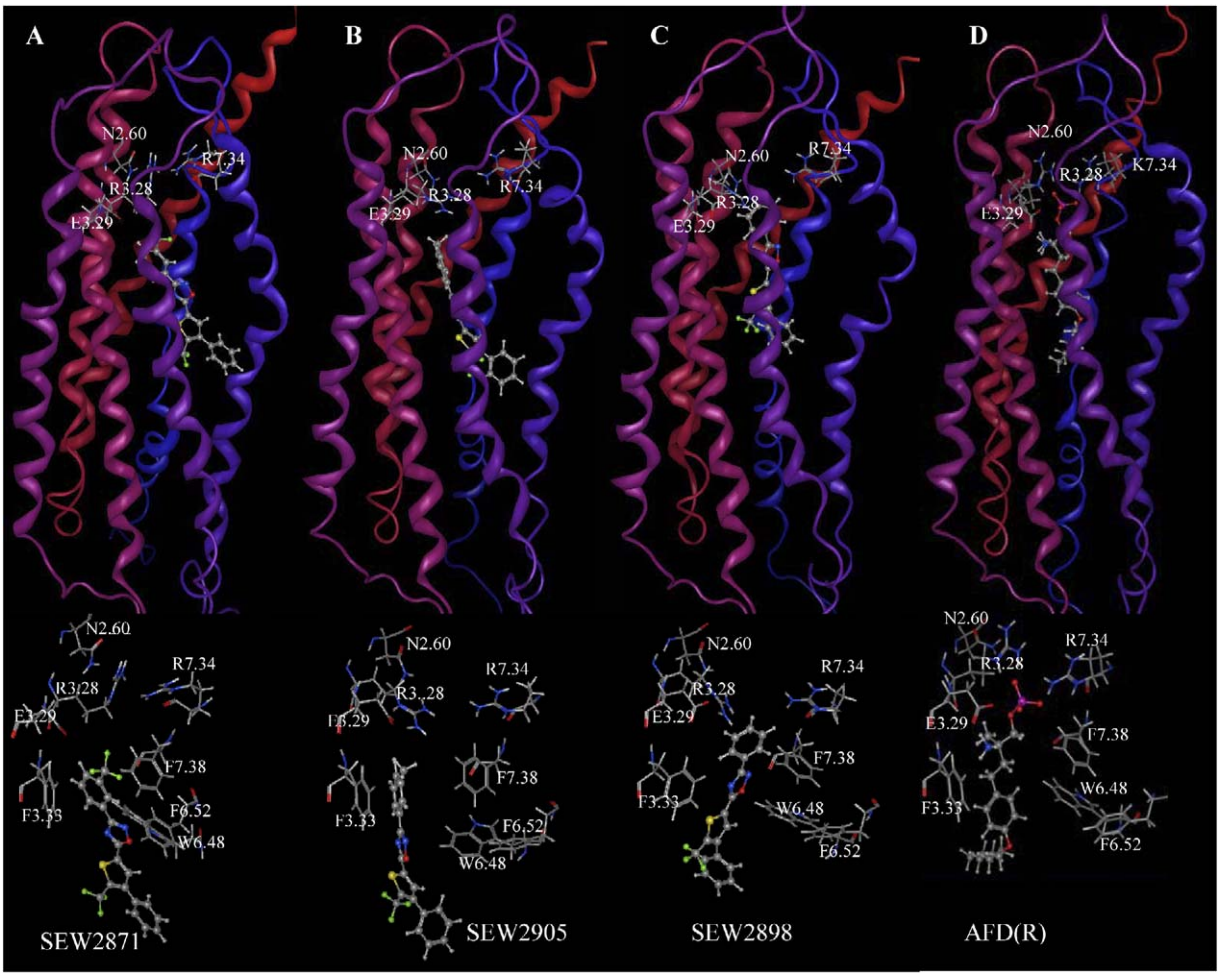

Figure 5. Computational Models of the Ligand Binding Pocket Illustrating Ligand-Receptor Interactions

Top panels show a receptor backbone with ribbon shaded from red at the amino terminal end to blue at the carboxy terminal end with select receptor residues shown as stick models and ligands shown as ball-and-stick models. Bottom panels show a closer view of ligand binding pocket with ligands shown as ball-and-stick models and select receptor residues shown as stick models. Top panels are shown from a common perspective to emphasize similarities and differences in ligand position in the different complexes. The bottom panels also share a common perspective that differs from the top in order to better show the ligand binding pocket. (A) $S1P_1$-SEW2871 complex. (B) $S1P_1$-SEW2905 complex. (C) $S1P_1$-SEW2898 complex. (D) $S1P_1$-AFD(R) complex.

paired ion-pairing interaction between $S1P_1$ and S1P causes defective downstream kinase activities (Figure 6A). AFD(R)-induced kinase activity was also dependent on these ion-pairing residues but to a lesser extent (Figure 6E). Interestingly, these ion-pairing defective mutants also showed less phosphorylation of ERK1/2 and Akt than the wild-type receptor upon stimulation with SEW2871 (Figure 6B), despite its different molecular structure, supporting the computational model (Figure 5A). This suggests that SEW2871 binds to the same ligand binding pocket of $S1P_1$ as S1P, and the same amino acid residues that participate in S1P headgroup interaction are engaged in the formation of $S1P_1$-SEW2871 complex.

To assess whether the dipole interactions could contribute to the potency of SEW2871 on the $S1P_1$ receptor signal generation, we tested the effect of SEW2871 analogs without the trifluoromethyl group on downstream kinase activities as well as GTPγ^{35}S assay. SEW2905 and SEW2898 (Figure 1C) had comparable EC_{50} values obtained by GTPγ^{35}S assay of 107 ± 45 nM for SEW2905 and 25 ± 23 nM for SEW2898 (compared to 14 ± 8 nM for SEW2871). The wild-type and control N2.60K mutant receptors responded to SEW2905 and SEW2898 stimulation (Figures 6C and 6D), with significant phosphorylation of ERK2 and Akt. This suggests that SEW2898 contains the minimum structural requirement for $S1P_1$ agonism. These analogs, however, showed different interactions with mutant receptors, compared to SEW2871. SEW2905 and SEW2898 require some headgroup binding elements in order to recruit significant kinase responses, specifically showing diminished Akt and ERK2 responses in the E3.29(121)A and R7.34(292)A mutants but not the R3.28(120)A mutant.

Discussion

$S1P_1$-Selective Agonist SEW2871 Activates ERK, Akt, and Rac Pathways

We have recently reported that agonism of $S1P_1$ receptor is sufficient to control lymphocyte recirculation, using $S1P_1$-selective agonist SEW2871 [24]. Studying

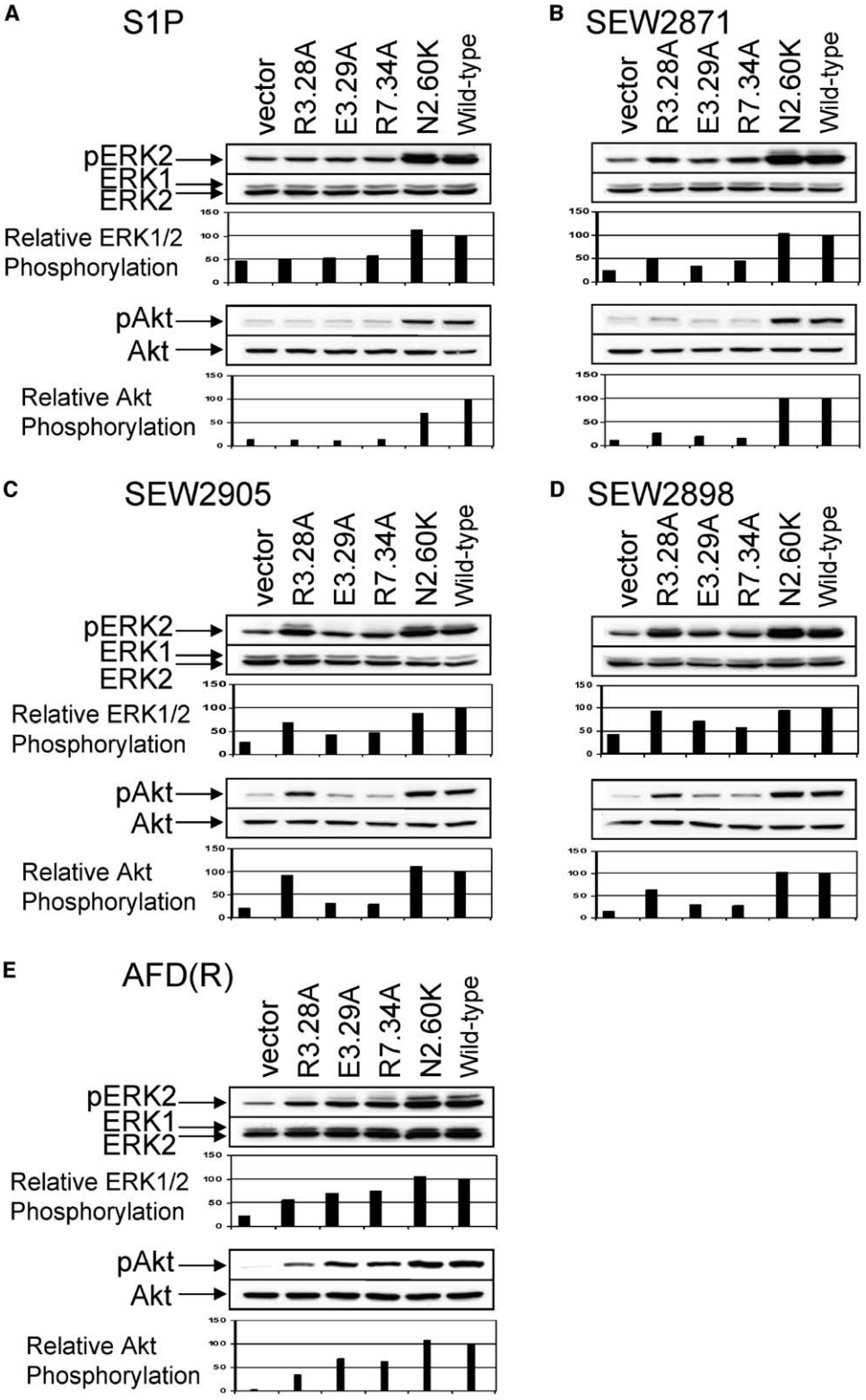

Figure 6. Polar Interaction between S1P$_1$ Receptor and Its Ligands Shown by Site-Directed Mutagenesis of the Ligand Binding Pocket

CHO cells were transfected with R3.28A, E3.29A, R7.34A, and N2.60K S1P$_1$. Cells were serum starved and stimulated with S1P 50 nM (A), SEW2871 500 nM (B), SEW2905 500 nM (C), SEW2898 500 nM (D), or AFD(R) 50 nM (E). Control cells treated with the vehicle (DMSO or methanol) showed only the minimal levels of pERK1/2 and pAkt (data not shown). Western blot analyses of phospho-ERK1/2, total ERK1/2, phospho-Akt, and total Akt levels are shown as representative autoradiograms of three independent experiments. The band intensities of phosphoproteins were integrated, normalized against total ERK or Akt, and expressed as percentage of the phosphorylation upon agonist stimulation of wild-type receptor (shown as 100%).

the downstream signals activated by natural and synthetic $S1P_1$ receptor ligands is important in understanding which potential signals may be responsible for discrete physiological and pharmacological effects of such ligands. Using the natural ligand S1P and the tetraaromatic $S1P_1$-selective agonist, SEW2871, we have shown that both ligands activate ERK, Akt, and Rac pathways in model cell lines transfected with a single subtype ($S1P_1$) of S1P receptors. Modeling and mutagenesis studies showed that SEW2871 shares significant overlap in receptor interactions with S1P, although their molecular structures are different from each other. Therefore, this study provides the first evidence that the structurally unrelated synthetic ligand can bind and activate $S1P_1$ through interaction similar to the natural ligand S1P.

Structure-Activity Relationships of $S1P_1$ Agonists Studied by Computational Modeling and Kinase Activation Downstream to $S1P_1$

A computational model of the $S1P_1$ receptor has been reported that predicts critical salt-bridge interactions of R3.28, E3.29, and R7.34 with S1P [31]. Subsequent examination of site-directed mutants of these residues by radioligand binding, ligand-induced [^{35}S]GTPγS binding, and receptor internalization assays confirmed the requirement of these residues for specific ligand recognition [31]. Docking of SEW2871 into the computational models of $S1P_1$ and $S1P_2$ revealed significant interactions with $S1P_1$ that overlap those of S1P, with regard to the volume and length of the hydrophobic interactions. It also suggests potential ion-dipole interactions between SEW2871 and the R3.28, R7.34, and E3.29 residues that support salt-bridge interactions with the aminophosphate headgroups of S1P (Figure 5A). In contrast, SEW2871 complex formation with $S1P_2$ was not supported (data not shown). One contributor to the selectivity difference is position 7.34, at which arginine appears only in the $S1P_1$ receptor.

Data derived from analysis of these $S1P_1$ receptor mutants showed that mutation of any of these three residues (R3.28, E3.29, or R7.34) significantly diminished the phosphorylation of both Akt and ERK2 by both S1P and SEW2871 (Figure 6A and 6B, respectively), providing formal evidence for an interaction between SEW2871 and the headgroup-coordinating residues, despite the chemical inability of SEW2871 to form salt-bridges with the receptor.

We further explored the headgroup interactions by studying the activation of kinases by analogs of SEW2871 that diminished the molecule's capability for making ion-dipole interactions by using the wild-type and the R3.28A, E3.29A, and R7.34A mutant receptors. The data confirmed the orientation of SEW2871 within the receptor and were consistent with amino-carboxylate analogs of SEW2871 [50]. Specifically, substitution of the electron-rich $-CF_3$ group with electron-poor $-CH_3$ (SEW2905; EC_{50}, 107 ± 45 nM in GTPγS binding) (Figures 1C and 6C) resulted in kinase activation that no longer depended upon R3.28 because of the disrupted ion-dipole interaction but was still abolished by R7.34A as well as by the E3.29A mutation.

Removal of the substituent from the D phenyl ring (SEW2898) (Figure 1C) resulted in a compound that is one bond length shorter than SEW2871 or SEW2905 and that retained the similar potency for $S1P_1$ (EC_{50}, 25 ± 23 nM in GTPγS binding). SEW2898 also showed somewhat limited headgroup dependency, resulting in a similar pattern of kinase activation to SEW2905. SEW2905 and SEW2898 may therefore define the aromatic-hydrophobic binding pocket within $S1P_1$ that does not depend upon R3.28 residue for the headgroup interaction and, thus, may serve as a useful probe to define the role of that residue in lymphopenia induction in future studies. In addition, the ion-dipole interaction of SEW2871 does not seem to be necessary for its potency in GTP binding and kinase activation because SEW2905 and SEW2898 without dipole moment were also potent agonists for $S1P_1$. The R3.28A mutant was activatable by SEW2905 and SEW2898 (Figures 6C and 6D), excluding the possibility that these mutations may cause a global disruption that makes the receptor unactivatable. In addition, proper folding and cell-surface expression of all the mutant receptors were confirmed by immunofluorescence of Flag tags [31].

$S1P_1$ Receptor Internalization and Recycling

S1P receptor agonists induced lymphopenia in vivo rapidly, inhibiting entry of bulk lymphocytes into lymph within an hour of ligand infusion, and continuous presence of agonist was required for maintenance of inhibition [24]. Therefore, ERK and Akt phosphorylation seems to be one of the early downstream effector pathways, and their temporary phosphorylation may be sufficient to activate further downstream effectors that are more directly involved in maintaining lymphopenia. However, it has been recently suggested that lymphopenia arises because of internalization and inactivation of $S1P_1$ upon FTY720-phosphate stimulation [25, 30]. Our data revealed that SEW2871 recapitulates the action of S1P in that both ligands induced receptor internalization and recycling (Figure 4). Both ligands were documented to induce a transient lymphopenia that persists only in the presence of ligand [24], and in the case of S1P, it requires less than 2-fold elevation in plasma S1P concentrations to induce lymphopenia [17]. On the other hand, FTY720-phosphate induced only internalization but not recycling. This raised a question whether FTY720-phosphate induces functional antagonism [30]. However, FTY720-phosphate and its analog AFD(R) induce alterations of lymphocyte trafficking at very low doses (ED50, 0.01 mg/kg) with free ligand concentrations in the low picomolar range [15]. Therefore, the lymphopenia induction with the substoichiometric receptor activation is most likely result from agonist effects but is unlikely to be functional antagonism.

Headgroup and Hydrophobic Interactions Contribute to the Potency of $S1P_1$ Agonists

SEW2871 has been shown to be a full agonist of $S1P_1$, inducing activation of $G_{i/o}$ to 100% of the response induced by the native agonist S1P, as measured by GTPγS binding [24]. However, its potency in receptor binding and downstream recruitment of the kinase signaling is significantly lower than the charged head-

group-containing ligands S1P or AFD(R). Kinase phosphorylation induced by AFD(R) (Figures 2A–2C and Table 1) had an EC_{50} approximately 3- to 10-fold less than that induced by S1P and may reflect the importance of the aromatic substituent within its acyl chain (Figure 1D). SEW2871 was measurably less potent at both G protein binding and kinase activation than AFD(R) and S1P (Table 1). SEW2871 was also less potent at Rac activation (Figure 3B). Therefore, the unique structure of SEW2871 provides this agonist with $S1P_1$-selectivity but with lower potency. This difference in potency in kinase activation is maintained in in vivo activity for the immunosuppression caused by lymphocyte sequestration.

At least three mechanisms may contribute to differences in potency of agonism downstream of $S1P_1$. These include different receptor conformations upon ligand binding, different rates of receptor activation/inactivation, and effects through transactivation of other signaling pathways. The enhanced potency of AFD(R) for G protein and kinase activation compared to S1P suggests that the aromatic component of the AFD tail (Figure 1D) may contribute to its higher potency. In this case, headgroup interactions are equivalent, and differences may reflect changes in receptor conformation [51] or rate of fractional occupancy.

The relatively low potency of SEW2871 on kinase activation may result from hydrophobic-aromatic interactions without headgroup salt-bridge interactions. This may reflect a slower fractional rate of receptor occupancy with ligands requiring complex hydrophobic-aromatic interactions. Conjugated aromatic systems like those present in the SEW2871 are not very flexible when compared to S1P or AFD(R). This lack of flexibility might influence the rate at which the ligands can access the buried binding pocket. A potentially slower on rate would not be as evident in GTPγS binding, an equilibrium measurement, but would be more apparent in kinetic interactions such as kinase activation or calcium flux.

An alternate explanation for the different potency of kinase recruitment may also reflect different degrees of pathway transactivation [42, 43]. GPCR-mediated activation of ERK/MAPK could occur through a number of pathways. It could take place either in a tyrosine kinase-independent pathway or in a tyrosine kinase-dependent pathway, which needs receptor tyrosine kinase transactivation [52]. In addition, GPCRs coupled to G protein can stimulate MAPK through phosphoinositide 3-kinase γ (PI3Kγ) in a Gβγ-dependent manner [53]. The relative importance of these multiple signaling tracks depends on cell type and receptor type [52] and possibly on agonist type. The presence of these multiple tracks for ERK signaling may also contribute to the differential potency of hydrophobic-aromatic $S1P_1$ agonist inducing kinase activation.

Different ligands thus interact differently with $S1P_1$ and induce signals with different potencies both in this model system, as well as in lymphocyte trafficking studies in blood, thymus [15], and lymph node in vivo [24]. The model system underestimates the potential complexities in vivo by not taking into account G protein promiscuity and tissue-dependent regulation of GPCRs by adaptors and by GTPases. Well-defined chemical probes of protein function will further the understanding of the molecular mechanisms underlying the different potencies of S1P receptor activation in both model systems and primary cells and tissues. These studies over time will shed light on mechanisms by which S1P receptors couple to multiple downstream effector functions and differentially regulate multiple physiological events. They will also provide a fundamental basis that could exploit these molecular systems on therapies for immune and cardiovascular diseases as well as cancer.

Significance

It is possible to define off-the-shelf compounds from high-throughput screening that replicate complex hydrophobic and headgroup interactions of natural ligands, activate multiple transduction pathways distal to their cognate receptor, provide structure-activity relationship, and allow chemical proof-of-concept in vivo. Specifically, the compound we identified was not only functionally S1P-like but also receptor subtype selective and did not require chemical optimization. In this study, we show that $S1P_1$-selective synthetic agonist SEW2871 activates G protein, ERK, Akt, and Rac pathways as well as $S1P_1$ internalization and recycling, recapitulating the action of the natural ligand S1P. Molecular modeling and receptor mutagenesis revealed that in addition to its proposed hydrophobic interactions with the receptor, SEW2871 requires the presence of polar receptor residues that support salt-bridge interactions with the S1P headgroup. Comparison of the natural ligand for $S1P_1$, S1P, with the synthetic agonists, SEW2871 and its analogs, illustrates significant contributions of headgroup interactions into the signal generation downstream of $G_{i/o}$ protein activation. These findings are of both fundamental and therapeutic importance. Sphingosine 1-phosphate (S1P) is a pleiotropic lysophospholipid that affects cell growth, cardiovascular function, and immune cell trafficking. Although we have begun to clarify mechanisms governing egress of lymphocytes from lymph nodes to lymph, the critical details of mechanism on the cellular level need to be resolved [24, 54]. Our data raise fundamental mechanistic questions of how ligands, such as S1P, AFD(R), and SEW2871, induce lymphopenia possibly through kinase and Rac activation. Our findings on SEW2871 and S1P agonism with receptor recycling suggest that functional antagonism may not be essential for induction of rapidly reversible lymphopenia. SEW2871 and its analogs shed light on properties of $S1P_1$ agonists necessary for the induction and maintenance of immunosuppression. Understanding the basis of $S1P_1$ receptor regulation of immune-cell trafficking will help developing selective immunotherapeutic treatment needed for autoimmune diseases and transplantation rejection.

Experimental Procedures

S1P Receptor Agonists

Sphingosine 1-phosphate (S1P) was purchased from BioMol (Plymouth Meeting, PA). SEW2871 (5-[4-phenyl-5-trifluoromethyl-thio

phen-2-yl]-3-[3-trifluoromethyl-phenyl]-1,2,4-oxadiazole), SEW2905 (3-[4-methylphenyl]-5-[4-phenyl-5-(trifluoromethyl)-2-thienyl]-1,2,4-oxadiazole), and SEW2898 (3-phenyl-5-[4-phenyl-5-(trifluoromethyl)-2-thienyl]-1,2,4-oxadiazole) were purchased from Maybridge (Tintagel, Cornwall, UK). AFD(R), phosphate ester of 2-amino-4-(4-heptyloxyphenyl)-2-methyl butanol, was a kind gift of Novartis Pharma (Basel, Switzerland, Volker Brinkmann).

Cell Culture and Transfection

Chinese hamster ovary (CHO) cells stably expressing human S1P receptors, $S1P_1$-CHO and $S1P_3$-CHO cells, were kindly provided by Danilo Guerini (Novartis Pharma). They were maintained in RPMI1640 (Life Technologies, Gibco) containing 10% fetal bovine serum, 0.5 mg/ml G418, 50 μg/ml gentamycin, 100 units/ml penicillin, 100 μg/ml streptomycin, and 10 mM HEPES. For the site-directed mutant-receptor study, CHO cells in a 6-well plate were transfected with 1 μg of plasmid DNA (pcDNA3 containing R3.28A, E3.29A, R7.34A, or N2.60K $S1P_1$ receptor construct as described [31]), 6 μl PLUS reagent, and 4 μl LipofectAMINE reagent (Life Technologies, Gibco). After 4 hr, the transfection medium was replaced with fresh medium. After 18 hr of growth, the transfected cells were serum starved for 6 hr and stimulated for 5 min with S1P, AFD(R), SEW2871, SEW2905, or SEW2898 diluted to various concentrations. Cells were lysed as follows for Western blotting. Transfection efficiency was measured in the cells on cover slips from a duplicate plate. The cells were fixed for 10 min with 4% paraformaldehyde in PBS, and excess paraformaldehyde was quenched with 50 mM NH_4Cl in PBS. Cells were then permeabilized for 30 min with 0.1% Triton X-100 in PBS and incubated for 30 min in blocking buffer (PBS, 0.1% Triton X-100, 5% BSA, 5% normal goat serum). Cells were subsequently incubated for 1 hr with anti-Flag antibody in PBS/0.1% Triton X-100/5% BSA/5% normal goat serum, rinsed in PBS/0.1% Triton X-100 three times, and incubated for 30 min in the dark with Alexa Fluor 488-conjugated goat anti-mouse IgG and Alexa Fluor 633-conjugated ToPro3 (Molecular Probes). Cells were rinsed three times, mounted, and viewed with an Olympus BX61 scanning confocal fluorescence microscope. All the mutant receptors were equivalently cell-surface expressed when examined for immunofluorescence of Flag tags as described [31].

Western Blotting

Control CHO cells and the CHO cells stably transfected with human $S1P_1$ or $S1P_3$ were cultured to 50% confluence on a 6-well plate in complete RPMI1640 supplemented with 10% FBS. Cells were serum starved for 16 hr and stimulated with S1P, AFD(R), or SEW2871 diluted to various concentrations in the serum-free medium with 0.1% fatty-acid-free BSA. At 5 min, 1 hr, or 4.5 hr, cells were lysed in 50 mM Tris (pH 8.0), 125 mM NaCl, 20 mM CHAPS, 2 mM dithiothreitol, 1 mM EDTA, 2 mM Na_3VO_4, 10 mM NaF, 1 mM PMSF, and protease inhibitor cocktail (Roche, Germany). For the study of pertussis toxin (PTx) inhibition, cells were incubated with PTx at the final concentration of 100 ng/ml for 3 hr, prior to agonist stimulation. Cell lysates were analyzed by Western blotting after separation on 10% SDS-PAGE with mouse monoclonal anti-phospho-ERK1/2 antibody (sc-7383; Santa Cruz Biotechnology) and rabbit polyclonal anti-phospho-Akt antibody (BD Biosciences). Total ERK1 and ERK2 were detected with a rabbit-affinity-purified polyclonal anti-ERK antibody (sc-94; Santa Cruz Biotechnology), and total Akt was detected with a rabbit-affinity-purified polyclonal anti-Akt1 antibody (BD Biosciences). Band intensities corresponding to pERK1, pERK2, and pAkt were quantitated by image analysis (Kodak 1D Scientific Imaging Systems). Amounts of pERK1/2 and pAkt were normalized for the total amounts of ERK1/2 and Akt.

Membrane Preparation and Receptor Activation Assay

Membranes were prepared from CHO cells expressing human $S1P_1$ for use in ligand and ^{35}S-GTPγS binding studies as described [17]. For ^{35}S-GTPγS binding assay, serial dilutions of S1P, AFD(R), SEW2871, SEW2905, or SEW2898 were added to membranes (1 to 10 μg protein/well) and assayed as described [17].

Receptor Binding Assay

[^{33}P]-S1P (final concentration of 83 pM) was added to serial dilutions of S1P or AFD(R) in a 96-well plate. Assays were initiated with the addition of 25 μg membrane protein of $S1P_1$-CHO cell membranes in a final volume of 200 μl assay buffer (50 mM HEPES [pH 7.5], 5 mM $MgCl_2$, 1 mM $CaCl_2$, 15 mM sodium fluoride, and 1% fatty-acid-free bovine serum albumin). Binding mixtures were incubated for 60 min at room temperature and terminated by filtration over Packard GF/B filter plates as described [54, 55].

Rac-Activation Assay

Cells were serum starved for 16 hr and stimulated with S1P (50 nM, 500 nM, or vehicle control) or SEW2871 (500 nM, 5 μM, or vehicle control) in the serum-free medium with 0.1% fatty-acid-free BSA. At 2 min and 5 min, cells were lysed in 500 μl ice-cold lysis buffer (50 mM Tris [pH 8.0], 500 mM NaCl, 0.5% NP-40, 1 mM EDTA, 1 mM $MgCl_2$, and protease inhibitor cocktail) containing 20 μg GST-tagged p21 binding domain of p21-activated protein kinase 1 (PAK1) [47]. The cell lysates were centrifuged at 16,000 × g at 4°C for 3 min, and 40 μl prewashed 50% GSH-Sepharose beads were added to the supernatant. The mixture was incubated at 4°C for 30 min, and the beads were washed twice in lysis buffer. The proteins bound to the beads were eluted with SDS sample buffer. Activated Rac GTPases were detected by Western blotting with a mouse monoclonal anti-Rac antibody (Upstate Biotech, Lake Placid, NY).

Receptor Internalization and Recycling

HEK293 cells that were stably transfected with GFP-tagged $S1P_1$ were grown in DMEM medium with 2% charcoal-stripped serum for 2 days [28]. Cells were pretreated with cycloheximide (15 μg/ml) for 30 min to block the synthesis of new $S1P_1$ and stimulated with 100 nM S1P, FTY720-phosphate, 500 nM SEW2871, or SEW2898 for 30 min. Cells were washed and replenished with plain DMEM and cycloheximide and incubated for indicated time points. The fluorescence of the recycled receptor at each time point was quantified and expressed as percent control.

Computational Homology Modeling

Residue Nomenclature

Amino acids within the transmembrane (TM) domains of $S1P_1$ and $S1P_2$ can be assigned index positions to facilitate comparison between receptors with different numbers of amino acids, as described by Weinstein and coworkers [56]. An index position is in the format x.xx. The first number denotes the TM domain in which the residue appears. The second number indicates the position of that residue relative to the most highly conserved residue in that TM domain, which is arbitrarily assigned position 50. E3.29, then, indicates the relative position of this arginine in TM 3 relative to the highly conserved arginine 3.50 in the E(D)RY motif [56].

Receptor-Model Development: $S1P_1$

A model of human $S1P_1$ (GenBank accession number AFP23365) was developed by homology to a model of rhodopsin (Protein Data Bank entry 1boj) in a manner described by Parrill and coworkers [31, 57]. Briefly, the rhodopsin model was used to generate TM1–TM6, whereas the structure for the seventh TM was based on TM7 of the dopamine D2 receptor model [58]. The preliminary model was further refined by converting all *cis* amide bonds to the *trans* configuration and by manually rotating side chains at polarity-conserved positions to optimize hydrogen bonding between TM. The AMBER94 force field [59] was utilized to optimize the receptor to a 0.1 kcal/mol · Å root mean square gradient.

Receptor-Model Development: $S1P_2$

A model of human $S1P_2$ (GenBank accession number AFP23365) was developed by homology to $S1P_1$. Alignment of the S1P receptor sequences was performed with the MOE software package (version 2003.01, Chemical Computing Group, Montreal, Canada). The alignment was optimized by the manual removal of gaps within the TM. A preliminary model was generated by homology modeling with default parameters and subsequently manually refined to optimize interhelical hydrogen bonding. *Cis*-amide bonds present in the loop regions were converted to the *trans* conformation by manual rotation followed by the minimization of two residues on either side of the amide bond to a root mean square (RMS) gradient of

0.1 kcal/mol · Å with the MMFF94 forcefield [60]. After these manual refinements, the entire receptor model was optimized with the MMFF94 forcefield to an RMS gradient of 0.1 kcal/mol · Å.

Ligand-Model Development

Computational models of SEW2871, SEW2905, and SEW2898 (Figure 1C) were built with the MOE software package. In order to maintain the delocalized pi stabilization of the ligand, rings B, C, and D remained coplanar throughout the docking calculation. The steric bulk associated with the thiophene CF_3 substituent prevents ring A from adopting a conformation that is coplanar with ring B; hence, there was free rotation of the bond between rings A and B. The MMFF94 force field was invoked for the subsequent geometry optimizations.

Docking

Using the AUTODOCK 3.0 software package [61], we docked the SEW2871 analogs into the $S1P_1$ and $S1P_2$ receptor models, and these complexes were evaluated based on electrostatic and other nonbonded interactions between the ligand and receptor. The complexes exhibiting the best interactions were geometry optimized with the MMFF94 force field [60], and the lowest energy complex after minimization was subjected to molecular dynamics simulations. Default docking parameters were used with the following exceptions: 3000 iterations were used in the local search phase, each of the 20 docking runs continued for 20,000 generations with a maximum of 1 × 109 energy evaluations.

Molecular Dynamics

An electrostatic potential for SEW2871 was derived from a quantum mechanical calculation at the HF/6-31G* level of theory. ANTECHAMBER used this restricted electrostatic potential to derive partial atomic charges compatible with the AMBER94 force field. A 500 ps molecular dynamics simulation was computed with the MOE software (NVT ensemble, 1 fs timesteps, 60 ps equilibration phase, 300 K), and the lowest energy complex was minimized with the AMBER94 force field. The optimized snapshot from the MD simulation is presented as the final model of the $S1P_1$ complex with SEW2871.

Supplemental Data

Supplemental Data include two figures and can be found with this article online at http://www.chembiol.com/cgi/content/full/12/6/703/DC1/.

Acknowledgments

We thank Dr. Jaewon Han for helpful advice on Rac activation study and Halley Nguyen for excellent technical assistance. This work was supported in part by National Institutes of Health R01 AI055509-01 to H.R. and National Institutes of Health R01 CA92160-01, HL61469, and the American Heart Association grant 0355199B to A.L.P. and G.T. The Chemical Computing Group generously donated the MOE program. E.J. acknowledges the Canadian Institutes of Health Research for the fellowship.

Received: November 16, 2004
Revised: March 16, 2005
Accepted: April 26, 2005
Published: June 24, 2005

References

1. Spiegel, S., and Milstien, M. (2003). Sphingosine 1-phosphate: an enigmatic signalling lipid. Nat. Rev. Mol. Cell Biol. *4*, 397–407.
2. Kluck, M.J., and Hla, T. (2002). Signaling of sphingosine-1-phosphate via the S1P/EDG-family of G-protein-coupled receptors. Biochim. Biophys. Acta *1582*, 72–80.
3. Siehler, S., and Manning, D.R. (2002). Pathways of transduction engaged by sphingosine 1-phosphate through G protein-coupled receptors. Biochim. Biophys. Acta *1582*, 94–99.
4. Spiegel, S., English, D., and Milstien, S. (2002). Sphingosine 1-phosphate signaling: providing cells with a sense of direction. Trends Cell Biol. *12*, 236–242.
5. Spiegel, S., and Milstien, S. (2002). Sphingosine 1-phosphate, a key cell signaling molecule. J. Biol. Chem. *277*, 25851–25854. Published online May 13, 2002. 10.1074/jbc.R200007200
6. Payne, S.G., Milstien, S., and Spiegel, S. (2002). Sphingosine-1-phosphate: dual messenger functions. FEBS Lett. *531*, 54–57.
7. Pyne, S., and Pyne, N.J. (2002). Sphingosine 1-phosphate signalling and termination at lipid phosphate receptors. Biochim. Biophys. Acta *1582*, 121–131.
8. Spiegel, S., and Milstien, S. (2000). Functions of a new family of sphingosine-1-phosphate receptors. Biochim. Biophys. Acta *1484*, 107–116.
9. Spiegel, S., and Milstien, S. (2003). Exogenous and intracellularly generated sphingosine 1-phosphate can regulate cellular processes by divergent pathways. Biochem. Soc. Trans. *31*, 1216–1219.
10. Sugiyama, A., Yatomi, Y., Ozaki, Y., and Hashimoto, K. (2000). Sphingosine 1-phosphate induces sinus tachycardia and coronary vasoconstriction in the canine heart. Cardiovasc. Res. *46*, 119–125.
11. Ohmori, T., Yatomi, Y., Osada, M., Kazama, F., Takafuta, T., Ikeda, H., and Ozaki, Y. (2003). Sphingosine 1-phosphate induces contraction of coronary artery smooth muscle cells via S1P(2). Cardiovasc. Res. *58*, 170–177.
12. Karliner, J.S. (2002). Lysophospholipids and the cardiovascular system. Biochim. Biophys. Acta *1582*, 216–221.
13. English, D., Brindley, D.N., Spiegel, S., and Garcia, J.G.N. (2002). Lipid mediators of angiogenesis and the signalling pathways they initiate. Biochim. Biophys. Acta *1582*, 228–239.
14. Garcia, J.G.N., Liu, F., Verin, A.D., Birukova, A., Dechert, M.A., Gerthoffer, W.T., Bamburg, J.R., and English, D. (2001). Sphingosine 1-phosphate promotes endothelial cell barrier integrity by Edg-dependent cytoskeletal rearrangement. J. Clin. Invest. *108*, 689–701.
15. Rosen, H., Alfonso, C., Surh, C.D., and McHeyzer-Williams, M.G. (2003). Rapid induction of medullary thymocyte phenotypic maturation and egress inhibition by nanomolar sphingosine 1-phosphate receptor agonist. Proc. Natl. Acad. Sci. USA *100*, 10907–10912. Published online September 3, 2003. 10.1073/pnas.1832725100
16. Xie, J., Nomura, N., Quackenbush, E., Forrest, M., and Rosen, H. (2003). Sphingosine-1-phosphate receptor agonists impair the efficiency of the local immune response by altering trafficking of naïve and antigen-activated CD4+ T cells. J. Immmunol. *170*, 3662–3670.
17. Mandala, S., Hajdu, R., Bergstrom, J., Quackenbush, E., Xie, J., Milligan, J., Thornton, R., Shei, G.-J., Card, D., Keohane, C., et al. (2002). Alteration of lymphocyte trafficking by sphingosine-1-phosphate receptor agonists. Science *296*, 346–349.
18. Brinkmann, V., Davis, M.D., Heise, C.E., Albert, R., Cottens, S., Hof, R., Bruns, C., Prieschl, E., Baumruker, T., Hiestand, P., et al. (2002). The immune modulator FTY720 targets sphingosine 1-phosphate receptors. J. Biol. Chem. *277*, 21453–21457.
19. Rosen, H., Sanna, M., and Alfonso, C. (2003). Egress: a receptor-regulated step in lymphocyte trafficking. Immunol. Rev. *195*, 160–177.
20. Igarashi, J., and Michel, T. (2000). Agonist-modulated targeting of the EDG-1 receptor to plasmalemmal caveolae. eNOS activation by sphingosine 1-phosphate and the role of caveolin-1 in sphingolipid signal transduction. J. Biol. Chem. *275*, 32363–32370.
21. Igarashi, J., and Michel, T. (2001). Sphingosine 1-phosphate and isoform-specific activation of phosphoinositide 3-kinase β. J. Biol. Chem. *276*, 36281–36288.
22. Dantas, A.P.V., Igarashi, J., and Michel, T. (2003). Sphingosine 1-phosphate and control of vascular tone. Am. J. Physiol. Heart Circ. Physiol. *284*, H2045–H2052.
23. Murata, N., Sato, K., Tomura, H., Kon, J., Yanagita, M., Kuwabara, A., Ui, M., and Okajima, F. (2000). Interaction of sphingosine 1-phosphate with plasma components, including lipoproteins, regulates the lipid receptor-mediated actions. Biochem. J. *352*, 809–815.
24. Sanna, M.G., Liao, J., Jo, E., Alfonso, C., Ahn, M.-Y., Peterson, M.S., Webb, B., Lefebvre, S., Chun, J., Gray, N., et al. (2004). Sphingosine 1-phosphate (S1P) receptor subtypes S1P1 and

S1P3, respectively. Regulate Lymphocyte Recirculation and Heart Rate. J. Biol. Chem. *279*, 13839–13848.
25. Matloubian, M., Lo, C., Cinamon, G., Lesneski, M., Xu, Y., Brinkmann, V., Allende, M., Proia, R., and Cyster, J. (2004). Lymphocyte egress from thymus and peripheral lymphoid organs is dependent on S1P receptor 1. Nature *427*, 355–360.
26. Allende, M.L., Dreier, J.L., Mandala, S., and Proia, R.L. (2004). Expression of the sphingosine-1-phosphate receptor, S1P1, on T-cells controls thymic emigration. J. Biol. Chem. *279*, 15396–15401.
27. Hale, J.J., Lynch, C.L., Neway, W., Mills, S.G., Hajdu, R., Keohane, C.A., Rosenbach, M.J., Milligan, J.A., Shei, G.J., Parent, S.A., et al. (2004). A rational utilization of high-throughput screening affords selective, orally bioavailable 1-benzyl-3-carboxyazetidine sphingosine-1-phosphate-1 receptor agonists. J. Med. Chem. *47*, 6662–6665.
28. Liu, C.H., Thangada, S., Lee, M.J., Van Brocklyn, J.R., Spiegel, S., and Hla, T. (1999). Ligand-induced trafficking of the sphingosine-1-phosphate receptor EDG1. Mol. Biol. Cell *10*, 1179–1190.
29. Kohno, T., Wada, A., and Igarashi, Y. (2002). N-glycans of sphingosine 1-phosphate receptor Edg-1 regulate ligand-induced receptor internalization. FASEB J. *16*, 983–992.
30. Graler, M.H., and Goetzl, E.J. (2004). The immunosuppressant FTY720 down-regulates sphingosine 1-phosphate G-protein-coupled receptors. FASEB J. *18*, 551–553. Published online January 8, 2004. 10.1096/fj.03-0910fje
31. Parrill, A.L., Wang, D., Bautista, D.L., Van Brocklyn, J.R., Lorincz, Z., Fischer, D.J., Baker, D.L., Liliom, K., Spiegel, S., and Tigyi, G. (2000). Identification of Edg1 receptor residues that recognize sphingosine 1-phosphate. J. Biol. Chem. *275*, 39379–39384.
32. Rosen, H., and Liao, J. (2003). Sphingosine 1-phosphate pathway therapeutics: a lipid-receptor paradigm. Curr. Opin. Chem. Biol. *7*, 461–468.
33. Kolesnick, R. (2002). The therapeutic potential of modulating the ceramide/sphingomyelin pathway. J. Clin. Invest. *110*, 3–8.
34. An, S., Zheng, Y., and Bleu, T. (2000). Sphingosine 1-phosphate-induced cell proliferation, survival, and related signaling events mediated by G-protein-coupled receptors Edg3 and Edg5. J. Biol. Chem. *275*, 288–296.
35. Pebay, A., Toutant, M., Premont, J., Calvo, C., Venance, L., Cordier, J., Glowinski, J., and Tence, M. (2001). Sphingosine-1-phosphate induces proliferation of astrocytes: regulation by intracellular signalling cascades. Eur. J. Neurosci. *13*, 2067–2076.
36. Wang, L., Cummings, R., Usatyuk, P., Morris, A., Irani, K., and Natarajan, V. (2002). Involvement of phospholipases D1 and D2 in sphingosine 1-phosphate-induced ERK (extracellular-signal-regulated kinase) activation and interleukin-8 secretion in human bronchial epithelial cells. Biochem. J. *367*, 751–760.
37. Harada, J., Foley, M., Moskowitz, M.A., and Waeber, C. (2004). Sphingosine-1-phosphate induces proliferation and morphological changes of neural progenitor cells. J. Neurochem. *88*, 1026–1039.
38. Kim, D.S., Hwang, E.S., Lee, J.E., Kim, S.Y., Kwon, S.B., and Park, K.C. (2003). Sphingosine-1-phosphate decreases melanin synthesis via sustained ERK activation and subsequent MITF degradation. J. Cell Sci. *116*, 1699–1706.
39. Tanimoto, T., Lungu, A.O., and Berk, B.C. (2004). Sphingosine 1-phosphate transactivates the platelet-derived growth factor beta receptor and epidermal growth factor receptor in vascular smooth muscle cells. Circ. Res. *94*, 1050–1058. Published online March 25, 2004. 10.1161/01.RES.0000126404.41421.BE
40. Davaille, J., Li, L., Mallat, A., and Lotersztajn, S. (2002). Sphingosine 1-phosphate triggers both apoptotic and survival signals for human hepatic myofibroblasts. J. Biol. Chem. *277*, 37323–37330. Published online July 22, 2002. 10.1074/jbc.M202798200
41. Lee, M., Thangada, S., Paik, J., Sapkota, G., Ancellin, N., Chae, S., Wu, M., Morales-Ruiz, M., Sessa, W., Alessi, D., et al. (2001). Akt-mediated phosphorylation of the G protein-coupled receptor EDG-1 is required for endothelial cell chemotaxis. Mol. Cell *8*, 693–704.
42. Igarashi, J., Erwin, P.A., Dantas, A.P.V., Chen, H., and Michel, T. (2003). VEGF induces S1P1 receptors in endothelial cells: implications for cross-talk between sphingolipid and growth factor receptors. Proc. Natl. Acad. Sci. USA *100*, 10664–10669.
43. Tanimoto, T., Jin, Z., and Berck, B. (2002). Transactivation of vascular endothelial growth factor (VEGF) receptor Flk-1/KDR is involved in sphingosine 1-phosphate-stimulated phosphorylation of Akt and endothelial nitric-oxide synthase (eNOS). J. Biol. Chem. *277*, 42997–43001.
44. Sanchez, T., Estrada-Hernandez, T., Paik, J., Wu, M., Venkataraman, K., Brinkmann, V., Claffey, K., and Hla, T. (2003). Phosphorylation and action of the immunomodulator FTY720 inhibits VEGF-induced vascular permeability. J. Biol. Chem. *278*, 47281–47290.
45. Connolly, J.O., Simpson, N., Hewlett, L., and Hall, A. (2002). Rac regulates endothelial morphogenesis and capillary assembly. Mol. Biol. Cell *13*, 2474–2485.
46. Takuwa, Y. (2002). Subtype-specific differential regulation of Rho family G proteins and cell migration by the Edg family sphingosine-1-phosphate receptors. Biochim. Biophys. Acta *1582*, 112–120.
47. Sugimoto, N., Takuwa, N., Okamoto, H., Sakurada, S., and Takuwa, Y. (2003). Inhibitory and stimulatory regulation of Rac and cell motility by the G12/13-Rho and Gi pathways integrated downstream of a single G protein-coupled sphingosine-1-phosphate receptor isoform. Mol. Cell. Biol. *23*, 1534–1545.
48. Ryu, Y., Takuwa, N., Sugimoto, N., Sakurada, S., Usui, S., Okamoto, H., Matsui, O., and Takuwa, Y. (2002). Sphingosine-1-phosphate, a platelet-derived lysophospholipid mediator, negatively regulates cellular Rac activity and cell migration in vascular smooth muscle cells. Circ. Res. *90*, 325–332.
49. Gonzalez, E., Nagiel, A., Lin, A.J., Golan, D.E., and Michel, T. (2004). Small interfering RNA-mediated down-regulation of caveolin-1 differentially modulates signaling pathways in endothelial cells. J. Biol. Chem. *279*, 40659–40669. Published online July 30, 2004. 10.1074/jbc.M407051200
50. Doherty, G., Forrest, M., Hajdu, R., Hale, J., Zhen, L., Mandala, S., Mills, S., Rosen, H., and Scolnick, E. July 2003. Selective S1P1/EDG1 receptor agonists. European patent WO03061567.
51. Yeagle, P.L., and Albert, A.D. (2003). A conformational trigger for activation of a G protein by a G protein-coupled receptor. Biochemistry *42*, 1365–1368.
52. Wetzker, R., and Bohmer, F.D. (2003). Transactivation joins multiple tracks to the ERK/MAPK cascade. Nat. Rev. Mol. Cell Biol. *4*, 651–657.
53. Lopez-Ilasaca, M., Crespo, P., Pellici, P.G., Gutkind, J.S., and Wetzker, R. (1997). Linkage of G protein-coupled receptors to the MAPK signaling pathway through PI 3-kinase gamma. Science *275*, 394–397.
54. Forrest, M., Sun, S.Y., Hajdu, R., Bergstrom, J., Card, D., Doherty, G., Hale, J., Keohane, C., Meyers, C., Milligan, J., et al. (2004). Immune cell regulation and cardiovascular effects of sphingosine 1-phosphate receptor agonists in rodents are mediated via distinct receptor subtypes. J. Pharmacol. Exp. Ther. *309*, 758–768. Published online January 27, 2004. 10.1124/jpet.103.062828
55. Candelore, M.R., Wright, M.J., Tota, L.M., Milligan, J., Shei, G.J., Bergstrom, J.D., and Mandala, S.M. (2002). Phytosphingosine 1-phosphate: a high affinity ligand for the S1P(4)/Edg-6 receptor. Biochem. Biophys. Res. Commun. *297*, 600–606.
56. Ballesteros, J.A., and Weinstein, H. (1995). Integrated methods for the construction of three-dimensional models and computational probing of structure-function relations in G protein-coupled receptors. Methods Neurosci. *25*, 366–428.
57. Bautista, D.L., Baker, D.L., Wang, D., Fischer, D.J., Van Brocklyn, J., Spiegel, S., Tigyi, G., and Parrill, A.L. (2000). Dynamic modeling of EDG1 receptor structural changes induced by site-directed mutations. J. Mol. Struct. THEOCHEM *529*, 219–224.
58. Konvicka, K., Guarnieri, F., Ballesteros, J.A., and Weinstein, H. (1998). A Proposed structure for transmembrane segment 7 of G protein-coupled receptors incorporating an asn-Pro/Asp-Pro motif. Biophys. J. *75*, 601–611.

59. Cornell, W.D., Cieplak, P., Bayly, C.I., Gould, I.R., Merz, K.M.J., Ferguson, D.M., Spellmeyer, D.C., Fox, T., Caldwell, J.W., and Kollman, P.A. (1995). A second generation force field for the simulation of proteins, nucleic acids, and organic molecules. J. Am. Chem. Soc. *117*, 5179–5197.
60. Halgren, T.A. (1996). Merck molecular force field. I. Basis, form, scope, parameterization, and performance of MMFF94. J. Comp. Chem. *17*, 490–519.
61. Morris, G.M., Goodsell, D.S., Halliday, R.S., Huey, R., Hart, W.E., Belew, R.K., and Olson, A.J. (1998). Automated docking using a Lamarckian genetic algorithm and an empirical binding free energy function. J. Comp. Chem. *19*, 1639–1662.